Impact of cellulose properties on its behavior in torrefaction: commercial microcrystalline cellulose versus cotton linters and celluloses extracted from woody and agricultural biomass

María González Martínez, Nathalie Marlin, Denilson da Silva Perez, Capucine Dupont, Carolina del Mar Saavedra Rios, Xuân-Mi Meyer, Christophe Gourdon, Gérard Mortha

Impact of cellulose properties on its behavior in torrefaction: commercial microcrystalline cellulose versus cotton linters and celluloses extracted from woody and agricultural biomass

María González Martínez (iD) · **Nathalie Marlin** · **Denilson Da Silva Perez** ·
Capucine Dupont · **Carolina del Mar Saavedra Rios** · **Xuan-Mi Meyer** ·
Christophe Gourdon · **Gérard Mortha**

Abstract Biomass composition on cellulose, hemicelluloses and lignin determinates its behavior in torrefaction (200–350 °C, default-oxygen atmosphere). Up to now, commercial microcrystalline cellulose was typically used to represent cellulose behavior in biomass torrefaction models based on macromolecular components. The objective of this work is to evaluate the impact of cellulose properties on its behavior in torrefaction, so as to identify the most suitable cellulose sample for modelling. To do this, five extracted celluloses from woody and agricultural biomass, commercial microcrystalline cellulose (Avicel) and four cotton linters tailored to different degrees of polymerization (DP) were considered. Cellulosic samples were deeply characterized in terms of fiber analysis, molar mass distribution (MMD), hydrodynamic behavior (SEC-RALS) and allomorphic structure. Cellulosic samples were torrefied in a thermogravimetric analysis up to two temperatures, leading to partial (300 °C) and total (350 °C) cellulose degradation. Extracted celluloses and Avicel cellulose degradation profiles showed strong differences at 300 °C. Polymer MMD,

M. González Martínez (✉)
IMT Mines Albi, RAPSODEE CNRS UMR-5302,
Université de Toulouse, Campus Jarlard,
81013 Albi Cedex 09, France
e-mail: maria.gonzalez_martinez@mines-albi.fr

N. Marlin · G. Mortha
CNRS, Grenoble INP, Institute of Engineering Univ.
Grenoble Alpes, LGP2, Univ. Grenoble Alpes,
38000 Grenoble, France

D. Da Silva Perez
InTechFibres Division, CS 90251, FCBA,
38044 Grenoble, France

C. Dupont
Department of Environmental Engineering and Water
Technology, IHE Delft Institute for Water Education,
Delft, The Netherlands

C. del Mar Saavedra Rios
CEA-LITEN, Laboratory of Bioresources Preparation
(LPB), Université Grenoble Alpes, 38000 Grenoble,
France

X.-M. Meyer · C. Gourdon
Laboratoire de Génie Chimique, Université de Toulouse,
CNRS, INPT, UPS, Toulouse, France

dispersity and the presence of residual hemicellulose sugars, especially xylose, strongly impacted cellulose degradation through torrefaction. Extracted celluloses presented high purity, narrow MMD and high DP, but a cellulose II structure due to mercerization. This cellulosic allomorph was shown to be more reactive, but it led to an identical final solid mass loss. The observed hydrodynamic behavior and the probable preservation of cellulose amorphous areas from native cellulose may also influence polymer structural behavior in torrefaction. Finally, at least one-order-of-magnitude DP variation was shown to be required to see an impact in cellulose degradation profile through torrefaction.

Introduction

Due to its high availability and its nature of neutral carbon fuel, biomass is a renewable source of energy that is expected to play an important role in the current global energetic transition (European Commission 2014). Thermochemical conversion routes were pointed out as convenient processes for the valorization of biomass and biowaste (Pisupati and Tchapda 2015; Vea et al. 2018). Among them, torrefaction is carried out at around 200 to 350 °C, under inert atmosphere, from several tens of minutes to one hour. It transforms biomass in a solid with upgraded properties, suitable for energetic applications, soil amendment or particle board manufacturing (Chen et al. 2015). In parallel, biomass torrefaction releases gaseous species, some of which are sources for "green chemicals" (Nocquet et al. 2014; Detcheberry et al. 2016).

A good knowledge of biomass structure, characteristics and properties is required to explain the phenomena associated to biomass transformation in torrefaction. In the literature, some studies proposed a first approach to biomass behavior in torrefaction through a linear combination of the behavior of its main macromolecular constituents, namely cellulose, hemicelluloses and lignin. In these studies, commercial compounds were typically used to represent biomass macromolecular components (Ramiah 1970; Yang et al. 2007; Chen and Kuo 2011a, b; Broström et al. 2012; Pasangulapati et al. 2012; Nocquet et al. 2014; Stefanidis et al. 2014). Such an approach should lead to some deviations from the expected behavior of a natural biomass that contains multi-interacting components. Indeed, interactions between the macromolecular constituents of biomass were shown to play a role at least at high temperatures and under moist atmospheres (Hosoya et al. 2007; Giudicianni et al. 2013).

Cellulose is the major structural component of cell walls, providing mechanical strength and chemical stability to lignocellulosic biomass (Sjöström 1993). It consists on a polysaccharide composed by (1,4)-D-glucopyranose monomeric units linked by a 1–4 β D-glycosidic bonds (Harmsen et al. 2010). In the case of native cellulose in biomass, the number-average degree of polymerization (DPn) may exceed 10 000, thus corresponding to a molar mass above 1.6×10^6 Dalton (Krässig 1993). Cellulose chains are linked together through extensive hydrogen bonding between hydroxyl groups, forming linear organized arrays of chains. This high degree of organization confers straightness to the structure and explains the relatively high crystallinity of cellulose microfibrils (Wang et al. 2013). The order in the glucan chains in the microfibrils is sometimes altered, leading to disordered areas along the length of microfibrils. These more likely-amorphous regions are suspected to be more propitious for the association of hemicelluloses with cellulose microfibrils (Gomez et al. 2008).

Cellulose polymer properties are a crucial factor determining its degradation pathway in torrefaction. Due to the complex structure of biomass, the easier way to study the effect of cellulose properties is by extracting it from biomass. Among the possible methods, the first step typically consists in a chlorite oxidation treatment of the raw biomass in slightly acidic conditions. This treatment is based on a selective oxidation and removal of lignin without impacting the cellulose polymer. Secondly, most of the hemicelluloses can be separated through an extraction step using dimethylsulfoxide (DMSO). The residual hemicelluloses remained in the solid matrix of the DMSO-extracted fraction can then be separated by an acid hydrolysis stage, so as to recover pure cellulose. The main advantage of this last acid hydrolysis stage is that it preserves the type I

allomorphic crystalline structure of the native cellulose. However, severe conditions for acid hydrolysis would lead to a more degraded cellulosic structure, with a considerable decrease of the degree of polymerization (DP) and partial loss of the cellulose amorphous regions. An alternative to acid hydrolysis consists of an alkaline solubilization of the residual hemicelluloses at high concentration of sodium hydroxide, named "hot" or "cold" caustic extraction stage (HCE or CCE, respectively), depending on the temperature of the process. This treatment is known to dissolve a significant part of the hemicelluloses and at least part of short cellulose chains. In the case of CCE, the mild temperature allows preserving the amorphous zones of the cellulose polymer, and short chains elimination leads to an increase of the average cellulose DP in the material. In the case of HCE, the well-known β-elimination reactions can occur, which is a major cause of polymer degradation. Moreover, in both cases, caustic extraction may change the cellulose crystalline structure to a type II, due to mercerization at ambient temperature which generally takes place at NaOH concentration above 8% (Kolpak and Blackwell 1976; Krässig 1993; Sixta 2008).

Cellulose degradation was deeply studied in the literature, frequently under pyrolysis temperatures (Katō and Komorita 1968; Ramiah 1970; Arseneau 1971; Broido and Nelson 1975; Bradbury et al. 1979; Agrawal 1988a, b; Kleen and Gellerstedt 1991; Pastorova et al. 1994; Luo et al. 2004; Wooten et al. 2004; Mamleev et al. 2007; Shen and Gu 2009; Shen et al. 2010; Wang et al. 2012; Paulsen et al. 2013). Macromolecular components behavior in torrefaction, including cellulose, gave rise to specific studies (Chen and Kuo 2011a, b; Nocquet et al. 2014; Chen et al. 2018). As a result, cellulose degradation was identified for starting at intermediate to high torrefaction temperatures, between 275 and 300 °C, and continues until 350 to 400 °C (Williams and Besler 1996; Biagini et al. 2006; Chen et al. 2015). These temperature ranges for cellulose transformation were identified by thermogravimetric analysis (TGA) of commercial microcrystalline celluloses, such as Avicel P101 and Sigmacell (Wang et al. 2012; Cheng et al. 2012). However, these cellulosic substrates present a higher crystallinity and a lower degree of polymerization than those found in native cellulosic substrates, due to their purification by acid hydrolysis. Such characteristics might impact their degradation

temperature range and profile, compared to those expected for native cellulose in biomass (Krässig 1993; Ioelovich and Leykin 2009; Sixta 2008).

The objective of this work was to evaluate the impact of cellulose properties on its behavior in torrefaction, so as to identify the most suitable cellulosic substrate(s) to represent cellulose in biomass torrefaction models. To do this, one commercial Avicel microcrystalline cellulose sample, four cotton linter samples (CL) and five cellulose samples extracted from woody and agricultural biomass species were chosen. The chemical treatments carried out in the extraction procedure were selected to obtain cellulose samples as close as possible to native cellulose in biomass. Furthermore, a sample of Avicel microcrystalline cellulose treated through CCE was also considered. All samples were deeply characterized through fiber analysis, molar mass distribution and allomorphic structure. In a second step, these cellulosic samples were torrefied in a thermobalance (TGA), in order to study the links between the degradation profiles and the cellulose sample properties.

Cellulosic materials

Extracted celluloses

Cellulose-based fractions were isolated through in-house developed methods from five biomass species from different biomass families:

- Coniferous wood: pine.
- Deciduous wood: ash wood and beech.
- Herbaceous crop: miscanthus.
- Agricultural residue: wheat straw.

Raw biomass samples were harvested in the South of France. Forestry biomass samples were received as woodchips and dried at 60 °C during 24 h. Herbaceous and agricultural biomass samples were received as pellets. Their moisture content was low and thus no extra drying was required. Biomass samples were then sampled following the standard XP CENT/TS 14780 and grinding using a laboratory 5-knife mill (Pulverisette) equipped with a 1 mm sieve. Extractives were removed using an ASE apparatus (Accelerated Solvent Extractor, Dionex Co.), firstly with water and

then with acetone. The extracted material was air-dried during one week prior its delignification using sodium chlorite. Then, a major part of the hemicelluloses was separated through a DMSO extraction stage. A cold caustic extraction stage (CCE; NaOH 2.5 M, 60 °C, 30 min) was then carried out on the secondary fraction of the DMSO extraction, so as to obtain the cellulose fraction. The extent of each step of the extraction procedure was defined by purity criteria and therefore adapted to each biomass type. As a result, each step may need slightly different reaction time for woody and agricultural biomasses, in function of the resilience of their structure. The details of this extraction procedure can be found in (González Martínez et al. 2020).

Commercial microcrystalline cellulose

One sample of commercial microcrystalline cellulose was studied to compare its torrefaction behavior to that of the extracted celluloses. Avicel PH-101 from Sigma Aldrich was used (product code 51710P06, CAS number 9004-34-6). It was received in the form of powder with a granulometry below 50 μm.

Avicel microcrystalline cellulose was used on its commercial form (sample named Avicel cellulose). Furthermore, a second sample was prepared from Avicel cellulose by a CCE stage under identical operating conditions to those for extracting cellulose fractions from biomass ("Extracted celluloses" section). This sample was named Avicel cellulose (after CCE).

Cotton linters

Several cotton linter pulp samples, representing a crystalline cellulose with a high purity, were prepared at different weight-average degrees of polymerization values (DPw = 757, 850, 865 and raw, 1937) by a patented oxidation process based on the use of ClO_2 and NaOH at various temperature and dosage. This process led to highly purified cellulosic fibers which kept the shape and morphology of the original bleached cotton linter fibers.

Experimental procedure

Cellulose characterization

Polysaccharide content

The elemental sugars content was measured for the extracted celluloses and Avicel cellulose samples through ion chromatography after a two-step hydrolysis of samples in sulfuric acid (TAPPI standard T249 cm-85), as described in (González Martínez et al. 2019).

Multi-detection size-exclusion chromatography (SEC-DRI-UV-LALS/RALS-viscometer)

Extracted celluloses, Avicel cellulose samples and cotton linter samples were characterized in terms of molar mass distribution (MMD) and hydrodynamic molecular parameters by means of a derivatization procedure leading to cellulose tricarbanilates (CTC's). It consists of a non-polar cellulose derivative fully soluble in THF (tetrahydrofuran), the chromatographic solvent used for the analysis of MMD by size-exclusion chromatography (SEC). Cellulose reaction with phenylisocyanate is well-known and it allows full derivatization of the hydroxyl groups borne by the cellulosic chains, i.e. a degree of substitution very close to three. Derivatization followed a procedure adapted from (Berggren et al. 2003). Three steps of solvent exchange with pure/dry dimethylacetamide (DMAC) were applied on the wet pulp sample (50 mg dry basis). After the last filtration step, the sample was transferred to a 150 mL reactor vessel in which an excess of DMAC-LiCl (6% LiCl) and phenylisocyanate were added simultaneously on the sample. The reaction was carried out at 40 °C under mild stirring during 5 days. It was stopped by adding an excess of methanol. Dilution in DMAC and final dilution in THF allowed reaching a CTC concentration of about 0.35 mg.mL^{-1} for SEC injection. In the case of Avicel cellulose samples, derivatization was carried out in pyridine instead of DMAc-LiCl, and no solvent exchange step was applied on the starting powder sample which was pre-dried at 60 °C.

The chromatographic system included a Malvern GPC-max/TDA 302 system equipped with DRI, UV, LALS, RALS and viscometer detectors, a set of three PL-GEL mixed-B columns, one PL-GEL guard

column, all kept in an oven at 35 °C. The system was eluted with THF at a flow rate of 1 mL.min^{-1}. Data were treated with the OMNISEC 4.5^{TM} software from Malvern Corporation. Molar mass (M) calculation of each eluent fraction was based on the coupling of DRI (differential refractometry) and LALS (low-angle light-scattering) signals. Coupling DRI and viscometer signals allowed determining the intrinsic viscosity [η], which knowing the value of M, resulted in the calculation of the hydrodynamic radius (R$_h$) of the polymer in the eluent slice by the Einstein law. The gyration radius was calculated from the Zimm plot based on coupling the DRI signal and the two-angle (low-angle, right-angle) light-scattering signals.

Measuring the polymer hydrodynamic parameters (intrinsic viscosity and gyration radius) contributed in the assessment of the flexibility of the cellulose chains, conditioned by their structural nature, morphology in the solvent and degree of reticulation. Intrinsic viscosity [η] is proportional to the molar volume of the solvated polymer, and its variation with chain length gives an idea of the freeness and flexibility of the polymer chains, also related to the existence of cross-links (or not). This latter behavior is also resumed by calculating the Mark-Houwink-Sakurada (MHS) parameters derived from the MHS curves, representing the relationship between log [η] and log M, as given by the equation:

$$\log_{10}[\eta] = \log_{10} K + \alpha \log_{10} M \quad (1)$$

The weight-average hydrodynamic radius (R$_h$) corresponds to the hydrodynamic polymer volume following Einstein's theory of flow, this is, to the radius of the equivalent sphere flowing in the solvent.

X-ray diffraction (XRD)

X-Ray diffraction characterizations of cellulose extracted fractions, raw biomass samples, cotton linters and Avicel cellulose samples were carried out in an XPERT-PRO MPD Diffractometer system with the measuring program from PANalytical. The selected anode material was copper, with a selected wavelength K$_\alpha$ (Cu) = 1.5419 Å. The reflection method was Bragg–Brentano type.

Cellulose torrefaction

Torrefaction experiments were carried out for all cellulosic samples in a thermogravimetric device (TGA, LABSYS evo DTA/DSC from SETARAM). About 20 ± 2 mg of sample was torrefied in a platinum crucible (4.4 mm diameter and 8.2 mm height) under a 50 mL.min^{-1} nitrogen flow. Each torrefaction experiment combined non-isothermal conditions from 200 to the end temperature, with a heating rate of 3 °C.min^{-1}, and an isothermal step at this end temperature for 30 min. Two different end temperatures were selected for torrefaction experiments, with two different objectives:

- Torrefaction until 300 °C: cellulose degradation is still under progress, so the addition of an isothermal step at this temperature is intended to discriminate samples with a close behavior.
- Torrefaction until 350 °C: cellulose degradation is (almost) completed, so the whole degradation curve can be observed.

These operating conditions ensure chemical regime during torrefaction experiments (González Martínez et al. 2016). Excellent repeatability was found for the TGA experiments with relative difference between repeated measurements lower than 1%.

Results and discussion

Cellulose characterization

Polysaccharide content

Extracted celluloses and Avicel cellulose samples were characterized in terms of polysaccharide type and content (Table 1).

The sugar distribution of the extracted cellulosic samples confirms their high purity in glucose, and thus in cellulose. Glucose is largely dominant and only minor amounts of mannose can be found in ash-wood and pine samples. The presence of mannose might be due to the difficulty to extract the glucomannans by the method used, especially in coniferous wood. Avicel microcrystalline cellulose presents a lower cellulose purity compared to the extracted celluloses, principally due to the presence of xylose from hemicelluloses (Scheller and Ulvskov 2010). However, the

Table 1 Monomer sugars distribution of extracted celluloses and of Avicel microcrystalline cellulose

% of the total monosugars	Wood and plant extracted cellulose					Avicel microcrystalline cellulose	Avicel cellulose (after CCE)
	Ash wood	Beech	Miscanthus	Pine	Wheat straw		
Glucose	98.2	100	100	99.1	100	96.1	100
Xylose	0	0	0	0	0	2.4	0
Mannose	1.8	0	0	0.9	0	1.5	0
Galactose	0	0	0	0	0	0	0
Arabinose	0	0	0	0	0	0	0

glucose content of Avicel cellulose (after CCE) is higher than for Avicel microcrystalline cellulose, which proves the efficacy of CCE in removing residual hemicellulose sugars to obtain an extracted cellulose pure in glucose. The polysaccharide content of cotton linter samples was not measured, as they are composed of glucose above 99% (Sczostak 2010).
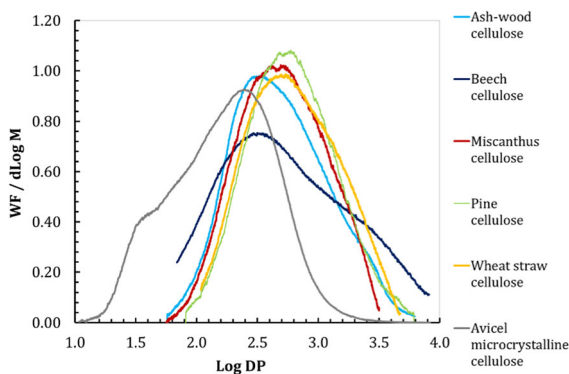
Cellulose molar mass distribution and hydrodynamic behavior

Extracted celluloses and Avicel microcrystalline cellulose The molar mass distribution (MMD) of each extracted cellulosic sample were firstly determined (Fig. 1). Avicel commercial microcrystalline cellulose was added to this analysis for comparison. Strong similarities were found for extracted celluloses from ash-wood, miscanthus, pine and wheat straw, which exhibit a relatively narrow MMD centered around $\log_{10}$ DP = 2.6

Fig. 1 Molar mass distribution (MMD) in function of the degree of polymerization (DP) of the extracted celluloses and Avicel microcrystalline cellulose (relative abundance curves)

(Mw = $\sim$ 65 kDa). However, in the case of beech cellulose, this distribution is considerably wider. This different MMD pattern may be attributed to the different behavior of the delignification treatment towards the beech wood, which will be discussed later. Comparatively, Avicel microcrystalline cellulose exhibits a broader MMD shifted towards lower DP values, with a local maximum at $\log_{10}$ DP = 2.4 (Mw = $\sim$ 40 kDa). This sample also presents a significant fraction of low mass molecules, represented by the second local maximum around $\log_{10}$ DP = 1.5 (Mw = $\sim$ 5 kDa). This fraction may correspond to small chains of degraded cellulose and residues of xylose and mannose hemicellulose sugars, according to the polysaccharide analysis (Table 1).

The weight-average degrees of polymerization (DPw) are the same order of magnitude for the five extracted celluloses ($\sim$ 400), while for the Avicel cellulose it is three to four times lower ($\sim$ 100, Table 2). This is also the case for the number-average degrees of polymerization (DPn), except for the beech cellulose, due to its wider MMD. These values agree with the peak DP values (DPp), which are slightly smaller for the hardwood compared to pine, miscanthus and wheat straw celluloses, but significantly higher than for the Avicel microcrystalline cellulose.

The dispersity $Đ_M$ of the cellulose polymer, represented by the ratio DPw/DPn, leads to the distinction of two families of extracted celluloses (Table 2): miscanthus, pine and wheat straw celluloses in the first group, and hardwood celluloses (ash-wood and beech) in the second one. The dispersity of the Avicel microcrystalline cellulose is between both families. The narrow MMD found for all biomass samples except beech is represented by their dispersity around 2. In the case of hardwoods, higher dispersity was

found even if polymer chain DP were slightly smaller (also confirmed by the DP at peak values). This different behavior might suggest the presence of small chains and/or of reticulations in the polymer, due to traces of residual hemicelluloses, which will be confirmed by the hydrodynamic parameters (see next paragraph). Finally, the Avicel microcrystalline cellulose exhibits a higher dispersity, principally caused by a MMD including two populations (lower and higher mass), the first one containing very degraded cellulose and small amounts of hemicelluloses chains.

Hydrodynamic parameters ($[\eta]$ and R_h) were also evaluated for extracted celluloses and Avicel microcrystalline cellulose (Table 3). They were close to each other for the extracted celluloses but more than twice the values for the Avicel microcrystalline cellulose. The higher R_h for beech cellulose, despite a rather low molar mass compared to the other samples, may be explained by the presence of small and long chains due to the high dispersity of the polymer. In the case of Avicel microcrystalline cellulose, the lower R_h and $[\eta]$ are in accordance with the shorter length of the cellulose chains.

The slope of the Mark-Houwink Sakurada (MHS) curves (a values in Table 3 and curve in Fig. 2) leads to distinguish two kinds of molecular behavior of the polymer in solution, as in the case of the mass-related parameters. Firstly, ash-wood and beech exhibit a-values between 0.7 and 0.8, considering the higher dispersity of beech cellulose. Secondly, miscanthus, pine and wheat straw cellulose values are close to 1. Avicel cellulose exhibits a particular behavior, with an a-value around 0.9. Hardwood-extracted samples (ash-wood and beech) are characterized by a higher dispersity and may have a higher probability of inter-chain cross-linking. The presence of small chains and cross-links probably limits the flexibility of the main cellulose chains and impacts the ability of the polymer to be volumetrically expanded (lower a-values). In the second case (agricultural biomass samples and pine) higher a-values, close to 1, might be explained by an effective extraction procedure which has fully removed small chains and cross-links, including most of hemicellulose residues, leading to a more homogeneous length and higher flexibility and freeness of the polymer chains. During acidic chlorite delignification the structure might conserve at least partially some small chains and cross-links linked to cellulose in the primitive biomass structure (Sixta 2008). In the case of

Avicel microcrystalline cellulose, the short length of the polymer chains favors an appreciable volumetric expansion of the polymer. However, the presence of hemicellulose residues and the mixture of different chain lengths rigidifies the structure and limits, to a certain extent, the flexibility of the chains.

As a summary, SEC characterizations would indicate that Avicel microcrystalline cellulose is significantly different and might be less representative of the native cellulose in biomass than the extracted celluloses, principally because of its much lower molar mass, presence of hemicellulose impurities and rather high dispersity, which affects the cellulose chains in their hydrodynamic behavior. Such characteristics result from the acid hydrolysis treatment utilized to produce this commercial cellulose. This treatment leads to a highly crystalline cellulosic structure, as it breaks cellulose chains in the amorphous areas, while crystalline regions remain unaffected (Krässig 1993). In the current study, the selected extraction procedure, which includes oxidation steps, solvent purification and alkaline extraction, lead to celluloses with higher molar mass values and narrower molar mass distributions, characterized by a low proportion of small chains, hemicellulose residues and inter-chain cross-links. These characteristics of the biomass extracted samples may suggest them as being more representative of the state of native cellulose in biomass or wood pulps, compared to commercial microcrystalline cellulose.

Cotton linters and Avicel cellulose samples In contrast to cellulosic materials originated from wood or agricultural biomass, cotton linters (CL) do not originally contain hemicelluloses. As in the former study, all cotton linters samples were characterized for their molar mass distribution (MMD) and hydrodynamic parameters by SEC-multidetectors. In this section, Avicel cellulose samples (microcrystalline and after CCE) were added for comparison.

As for the previously studied extracted celluloses fractions, a relatively narrow MMD was found for CL samples, centered at around $\log_{10}$ DP = 2.9 ($\sim$ 130 kDa) for the processed samples, and at $\log_{10}$ DP = 3.2 ($\sim$ 255 kDa) for the raw cotton linter sample, which fits the order of magnitude of the DPw of purified commercial cotton linters pulps (Table 2). This again contrasts with the two local

Table 2 Degree of polymerization and dispersity of extracted celluloses, Avicel cellulose (microcrystalline and after CCE) and cotton linters

Parameters	Wood and plant extracted cellulose					Avicel microcrystalline cellulose	Avicel cellulose (after CCE)	Cotton linters (CL)			
	Ash wood	Beech	Miscanthus	Pine	Wheat straw			DPw = 1937 (raw)	DPw = 865	DPw = 850	DPw = 757
DPn	341	320	368	441	453	103	96	829	446	447	388
DPw	744	1084	688	849	883	254	212	1937	865	850	757
DPp[a]	375	440	498	590	544	249	203	1572	660	662	587
$Đ_M = DPw/DPn$	2.18	3.39	1.87	1.92	1.95	2.46	2.22	2.34	1.94	1.90	1.95

[a]DP at peak refers to the DP observed at the top of the concentration peak in the DRI chromatogram

Table 3 Hydrodynamic parameters of extracted celluloses, Avicel cellulose (microcrystalline and after CCE) and cotton linters

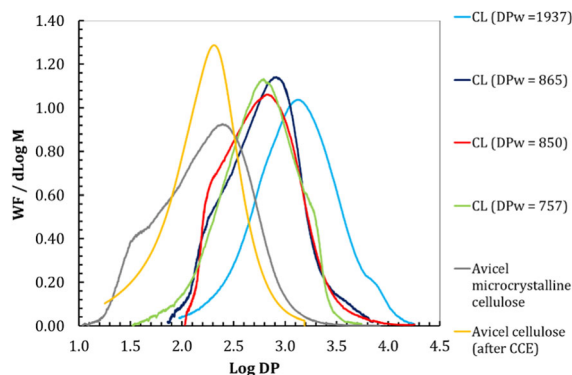| Parameters	Units	Wood and plant extracted cellulose					Avicel microcrystalline cellulose	Avicel cellulose (after CCE)	Cotton linters (CL)			
		Ash wood	Beech	Miscanthus	Pine	Wheat straw			DPw = 1937 (raw)	DPw = 865	DPw = 850	DPw = 757
η	mL/g	167.2	270.8	258.3	284.9	254.6	93.4	72.0	500	241	226	197
R_h	nm	20.1	26.5	23.6	26.5	25.9	11.5	10.3	40	24	23.3	21.8
Mark–Houwink–Sakurada parameters (MHS)												
a	–	0.748	0.798	0.917	0.961	1.082	0.909	0.849	0.784	0.852	0.862	0.803
Log K	–	– 3.899	– 4.088	– 4.668	– 4.951	– 5.724	– 4.657	– 4.398	– 3.990	– 4.419	– 4.467	– 4.166
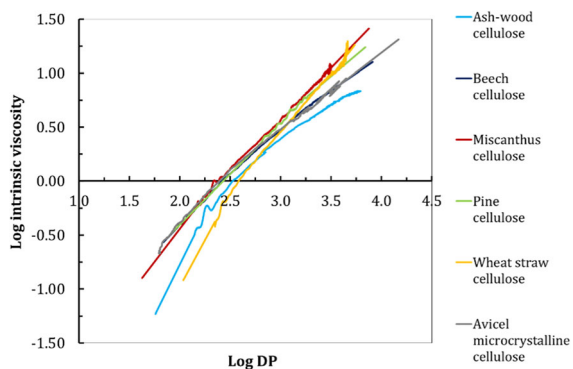
Fig. 2 Mark–Houwink–Sakurada curves (MHS curves) in function of the degree of polymerization of the extracted celluloses and Avicel microcrystalline cellulose

Fig. 3 Molar mass distribution (MMD) in function of the degree of polymerization (DP) of the cotton linters (CL) and of the Avicel cellulose samples (relative abundance or differential curves)

Fig. 4 Mark–Houwink–Sakurada curves (MHS curves) in function of the degree of polymerization of the cotton linters (CL) and the Avicel cellulose samples

maxima found for the Avicel microcrystalline cellulose MMD at lower DP values ($\log_{10}$ DP = 2.4 and 1.5). In the case of Avicel cellulose (after CCE), the first peak corresponding the low DP chains and residual hemicellulose sugar disappeared and a narrow MMD is found, centered around $\log_{10}$ DP = 2.3 ($\sim$ 30 kDa). This proves the efficacity of CCE in removing not only residual hemicellulose sugars, but also cellulose small chains and cross-links.
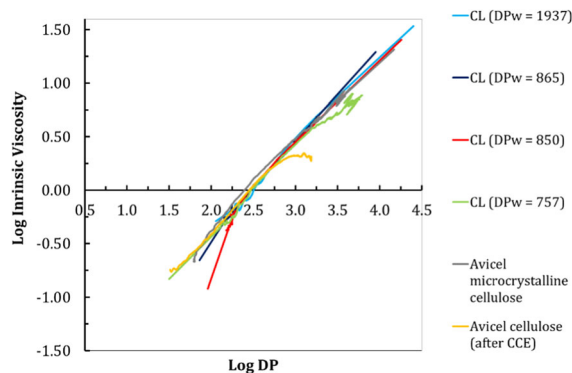
The average DP values (DPn, DPw, Table 2) were also found close to each other for all processed CL samples, but different of that of the raw CL sample (DPw = 1937). This might be due to the slight reduction in cellulose chain length due to CCE, as observed for the Avicel cellulose samples before and after this treatment. In all cases, average DP of CL samples remain between 3 times (DPw = 757) and 8 times (raw CL) higher than those for both Avicel cellulose samples.

The dispersity $Đ_M$ of the cellulose polymer, represented by the ratio DPw/DPn, was higher and close for the raw CL sample, beech cellulose and Avicel microcrystalline cellulose, due to their larger MMD. The three processed CL samples exhibit lower values, in agreement with their narrower MMD, while Avicel cellulose (after CCE) presents an intermediate behavior (Fig. 3).

Hydrodynamic parameters were also analyzed for CL samples. The logarithmic representation of the hydrodynamic radius (R_h) versus the molar mass exhibits a quite linear and regular curve (Fig. 4). The R_h value for the raw CL sample is about 2 to 2.5 times higher than that of the processed CL samples (Table 3),

which agrees with the predominance of polymer chains of about half the length of those in the raw CL sample. The value for the Avicel cellulose is about 5 times lower than that of the raw CL sample, which can again be explained by the strong depolymerization occurring during the acid hydrolysis process used to produce Avicel microcrystalline cellulose. This comparison is also consistent with the comparison of R_h values. Similar hydrodynamic parameters were measured for both Avicel cellulose samples, indicating any significant influence of CCE in this sense (Table 3).

Concerning calculated Mark-Houwink-Sakurada parameters (Table 3), the values for the processed CL samples seem intermediate between those of raw CL sample and Avicel cellulose samples. However, the good superimposition of the curves in Fig. 4 definitely indicates non-significant differences

between all samples in terms of hydrodynamic behavior.

As a summary, the SEC-multidetectors characterization of CL of different DPw (raw and processed samples) revealed narrow MMD and high molar mass values, which is an indicator of high purity, compared to Avicel microcrystalline cellulose. Furthermore, it was shown that CCE treatment efficacy removes cellulose small-chains and cross-links, as well as residual hemicellulose sugars.

Allomorphic structure

XRD characterizations were carried out on extracted celluloses, Avicel cellulose samples and CL samples (Fig. 5). They evidenced the mercerization of cellulose due to the CCE stage in the extraction procedure. As a result, cellulose allomorphic structure of type II was detected in extracted celluloses and Avicel cellulose after CCE (Fig. 5, right). Samples which were not treated through CCE, *i.e.* Avicel microcrystalline cellulose and CL samples, keep an allomorphic structure of type I (Fig. 5, left). This structure corresponds to that of native cellulose in raw biomass (Supplementary material, Fig. S1).

Cellulose torrefaction

Extracted celluloses and Avicel microcrystalline cellulose

Weight percentage moisture free remaining solid mass (%wmf) and degradation rates (%wmf.min^{-1}) versus temperature and time were measured for the extracted celluloses and for the Avicel microcrystalline cellulose in torrefaction until 300 °C (Fig. 6) and 350 °C (Fig. 7). The objective of this study is to evaluate the influence of the biomass type on the nature of the extracted cellulose sample and thus its behavior in torrefaction. Furthermore, they behavior will be compared to that of commercial microcrystalline cellulose, which was typically selected as representative of cellulose behavior in torrefaction models in the literature.

Solid degradation profiles (Fig. 6) appear to be similar for the five extracted celluloses, ash-wood and wheat straw cellulose being very close. The acceleration in the degradation rate of these celluloses is progressive from early torrefaction temperatures (around 220 °C), while an appreciable degradation of Avicel microcrystalline cellulose only started around 280 °C. Avicel microcrystalline cellulose degradation strongly accelerates and reaches a maximum during the 300 °C isothermal step, this maximum being at higher rates (2.5% wmf.min^{-1}) than those for extracted celluloses (around 1.0% wmf.min^{-1}). The degradation rate of Avicel microcrystalline cellulose strongly decelerates after the maximum, accompanied by a strong mass loss at 300 °C. On the contrary, the degradation of extracted celluloses in the isothermal step is only very few decelerated for wood celluloses and slightly more decelerated for agricultural celluloses. The final solid mass loss was lower for extracted celluloses (around 40%wmf) compared to that of Avicel microcrystalline cellulose (around 58%wmf).

At 350 °C, the remaining solid mass profiles are globally similar for all extracted celluloses (Fig. 7). As in the previous case, thermal decomposition starts from temperatures close to 200 °C for all samples. Then, it progressively accelerates around 300 °C. Degradation rate profiles reach a maximum at around 330 °C, slightly higher for beech and pine cellulose (around 6.5%wmf.min^{-1}) compared to the other samples (around 5.5%wmf.min^{-1}). A final solid mass loss from around 72%wmf is achieved for all extracted cellulose samples.

The degradation of Avicel microcrystalline cellulose starts again from higher temperatures (around 280 °C) than the extracted celluloses (around 220 °C). However, the acceleration of its degradation starts at lower temperatures and thus the maximum degradation rate is reached 10 °C earlier, at around 320 °C. This maximum (8.3%wmf.min^{-1}) is again higher than those of the extracted celluloses.
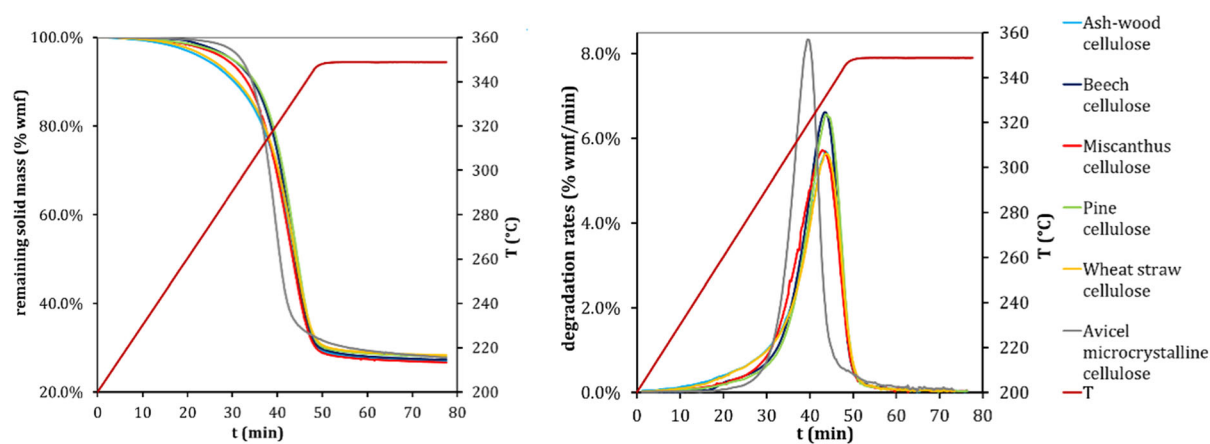
The obtained results for Avicel microcrystalline cellulose are in agreement with those of previous studies indicating that cellulose degradation rather starts at 300 to 350 °C (Williams and Besler 1996; Biagini et al. 2006). However, the degradation of all extracted celluloses starts from lower temperatures. Furthermore, the decomposition profiles are different to that of Avicel microcrystalline cellulose (Figs. 6 and 7). The reasons of these differences will be discussed later and linked to cellulose sample properties.
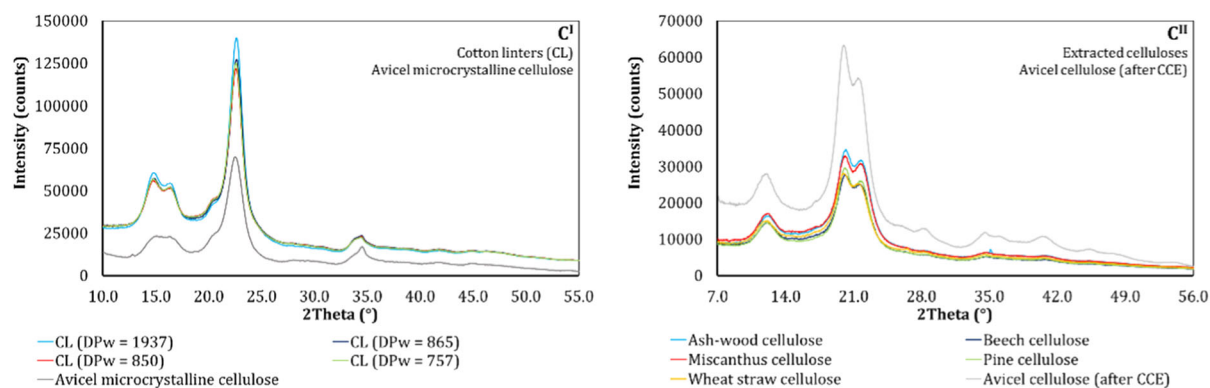
Fig. 5 XRD diffractograms: cotton linters and Avicel microcrystalline cellulose (left); extracted celluloses and Avicel cellulose (after CCE, right)
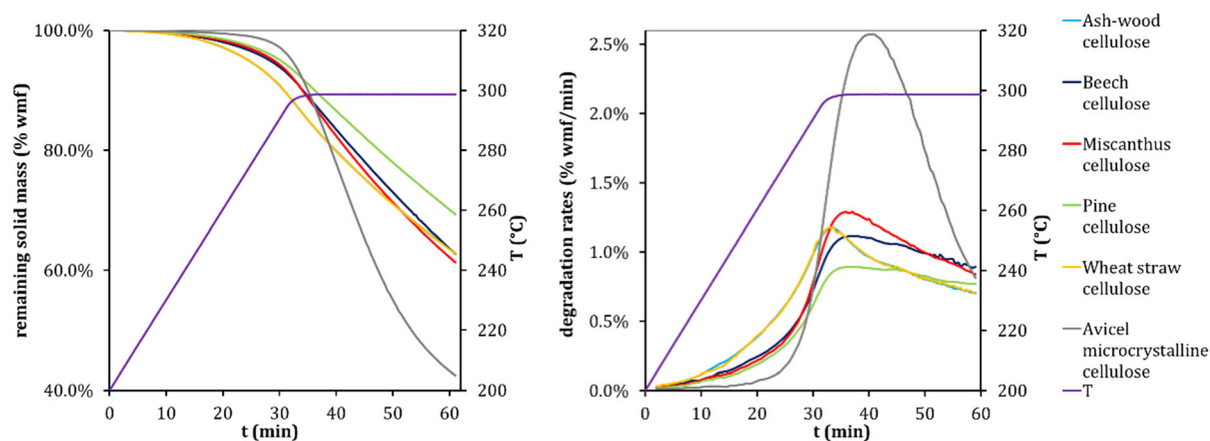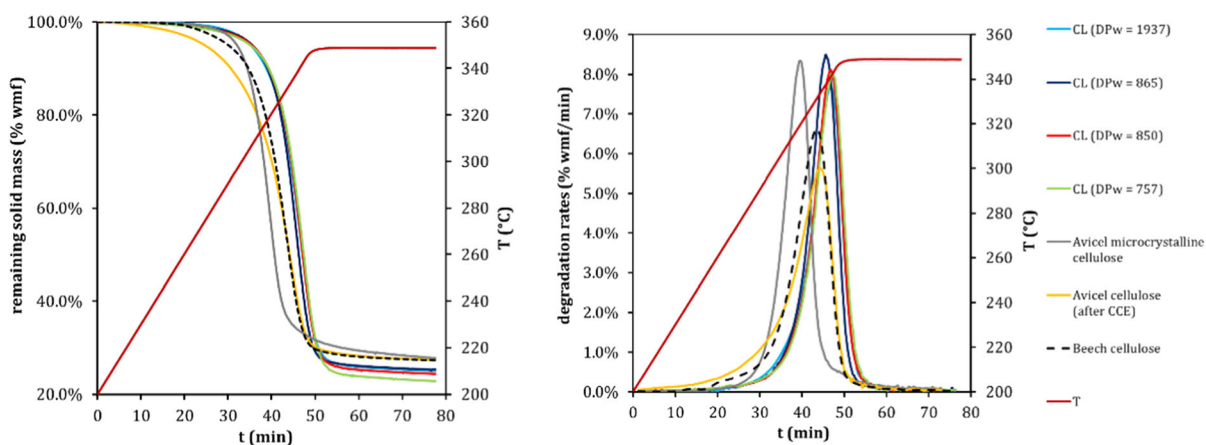

Fig. 6 Remaining solid mass (left) and degradation rates (right) versus temperature and time obtained for extracted celluloses and for Avicel microcrystalline cellulose in torrefaction in TGA-GC/MS until 300 °C

Fig. 7 Remaining solid mass (left) and degradation rates (right) versus temperature and time obtained for extracted celluloses and for Avicel microcrystalline cellulose in torrefaction in TGA-GC/MS until 350 °C
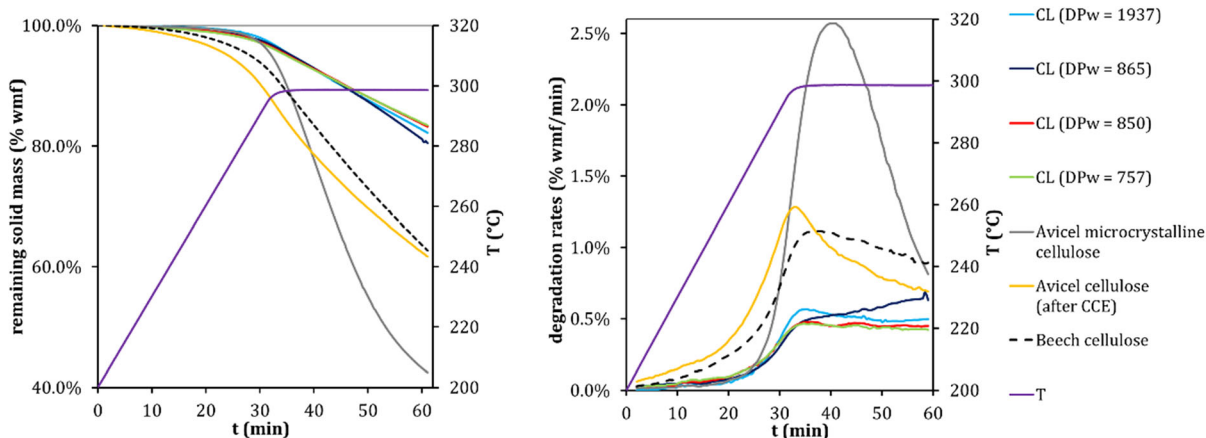
Fig. 8 Remaining solid mass (left) and degradation rates (right) versus temperature and time obtained for cotton linters (CL), Avicel cellulose samples and beech cellulose in torrefaction in TGA-GC/MS until 300 °C

Fig. 9 Remaining solid mass (left) and degradation rates (right) versus temperature and time obtained for cotton linters (CL), Avicel cellulose samples and beech cellulose in torrefaction in TGA-GC/MS until 350 °C

Cotton linters and Avicel cellulose samples

Solid degradation kinetics of cotton linter (CL) samples and Avicel cellulose samples (microcrystalline and after CCE) were analyzed in torrefaction in TGA until 300 °C (Fig. 8) and 350 °C (Fig. 9). Beech extracted cellulose was also added for comparison. This study follows several objectives:

1. evaluate the influence of the DP of cellulosic samples made of pure cellulose I on their torrefaction behavior by comparing the processed CL samples originated from the same raw pulp;
2. comparing CL and Avicel microcrystalline cellulose, both composed of cellulose I with a high

degree of crystallinity but a different purity on glucose;
3. comparing Avicel cellulose (after CCE) and beech extracted cellulose, both composed of cellulose II;
4. evaluate the effect of the allomorphic structure, cellulose I or cellulose II, by comparing Avicel cellulose samples: raw (commercial microcrystalline sample) and after CCE.

Below 300 °C, similar starting degradation temperature and shape of the degradation profiles are shown for cotton linters and Avicel microcrystalline cellulose on the one hand, and beech cellulose and Avicel cellulose (after CCE) on the other hand (Fig. 8). The degradation profiles of the 4 CL samples are very similar, except at 300 °C, where the

degradation rate of the raw CL seems to be slightly higher. In the isothermal step at 300 °C, the degradation profiles of all samples present a similar shape, except that of Avicel microcrystalline cellulose. Moreover, significant differences appear: while CL degradation rate is rather low and constant (around 0.5%wmf.min^{-1}), Avicel microcrystalline cellulose degradation rate is characterized by a large peak (2.5%wmf.min^{-1}) and then strongly decreases. Avicel cellulose (after CCE) presents a narrower maximum at half of the degradation rate of the untreated sample (1.3%wmf.min^{-1}). Beech extracted cellulose behavior is close to that of cotton linters, showing a maximum (1.3%wmf.min^{-1}) and then smoothly decreasing its degradation rate. Final solid mass loss is around 20%wmf for CL samples, 40%wmf for beech cellulose and Avicel cellulose (after CCE) and around 60%wmf for Avicel microcrystalline cellulose.

In torrefaction up to 350 °C, degradation profiles were similar for all samples (Fig. 9), characterized by a later starting degradation temperature and then a faster acceleration in the degradation for cellulose I type samples (CL and Avicel microcrystalline cellulose) compared to cellulose II type samples (beech extracted cellulose and Avicel cellulose, after CCE). In all cases, the maximum degradation rate is reached before the isothermal step, at 320 °C for Avicel microcrystalline cellulose, 330 °C for beech extracted cellulose and Avicel cellulose (after CCE) and 340 °C for cotton linters. Then, the degradation decelerates until values near to zero before the end of the experiment, without any profile change at the isothermal step. This leads to complete peaks where the whole degradation is observed. The maximum degradation rate for beech extracted cellulose and Avicel cellulose (after CCE) is lower (around 6%wmf.min^{-1}) than that of CL and Avicel microcrystalline cellulose (around 8%wmf.min^{-1}). A final solid mass loss of around 78%wmf was reached for all CL samples, while it was around 72%wmf for the other cellulosic samples.

Comparison of cellulose properties and behavior in torrefaction

In this section, the behavior in torrefaction of the different cellulosic samples ("Cellulose torrefaction" section) will be discussed according to the characterization carried out ("Cellulose characterization"

section), as well as to previous studies in the literature. Table 4 summarizes the main characteristics for each cellulosic sample type compared to those reported for native cellulose from biomass. At the same time, it proposes a categorization of the influence of cellulose properties on its behavior in torrefaction according to the results of the present study.

Biomass type

Any significant difference was observed between cellulose samples extracted from different woody and agricultural biomass species. As a result, one of these samples can be selected as representative of the behavior of extracted cellulose (through CCE) from biomass. This result agrees with previous studies in the literature, which showed that, contrarily to hemicelluloses and lignin in lignocellulosic biomass, cellulose generally presents a low structural variability (Krässig 1993).

Allomorphic structure

A different starting temperature for cellulose degradation in function of the allomorphic structure was observed in both torrefaction experiment until 300 and 350 °C. Cellulose II samples (extracted celluloses and Avicel cellulose after CCE) start their degradation at temperatures close to 200 °C, while this temperature is around 280 °C for cellulose I samples. A second difference is the lower maximum degradation rate for cellulose II samples compared to cellulose I ones, probably linked to the fact that they start degrading from lower temperatures. As a result, the area below the degradation rate curve for cellulose I and II samples appears to be close, as well as the final solid mass loss at 350 °C. This may indicate a higher reactivity of cellulose II in torrefaction, as its thermal decomposition occurs from lower temperatures (Pena et al. 2019). However, this higher reactivity does not present a significant impact in the final mass loss of cellulose.

Polysaccharide composition

All cellulosic samples analyzed present a high glucose content, which is close to 100% for most of the extracted celluloses (residual mannose measured in ash-wood and pine cellulose) and Avicel cellulose

Table 4 Comparison of the properties of native cellulose (from literature), extracted celluloses, commercial microcrystalline cellulose and cotton linters and their influence in cellulose torrefaction according to the results of the present study

Sample properties	Native cellulose[a]	Extracted celluloses	Avicel commercial microcrystalline cellulose	Cotton linters (CL)	Influence in torrefaction	Suspected influence in torrefaction
Glucose content	100%	98–99%	∼ 96%	∼ 100%	High	Higher reactivity at 300 °C with residual hemicellulose sugars (especially xylose). No influence of the biomass type
Impurities of hemicellulose sugars	Traces	(very low) xylan/mannan	∼ 4% xylan/mannan	Traces		
Molar mass distribution (MMD)	Narrow	Narrow	Wide (2 maxima)	Narrow	High	Smaller cellulose chains shift TGA degradation peak to lower temperatures
Dispersity $Đ_M$, (DPw/DPn)	1.2 to 2.2	∼ 2[b]	∼ 2.5	∼ 2		
Mass-average molar mass (Mw)	∼ 2 000 kDa	125—200 kDa	∼ 50 kDa	125—325 kDa	Intermediate	Lower DP slightly shifts the starting degradation temperature to lower values
Degree of polymerization (DPw)	∼ 10 000	∼ 400	∼ 100	∼ 1 600—700	Intermediate[c]	
Hydrodynamic behavior	n.d.[d]	Variable	Rigidity (cellulose and xylan short chains)	Certain flexibility	Low	Lower proportion of small chains, hemicellulose residues and inter-chain cross-links higher polymer flexibility and volumetric expansion (influence on polymer structure reaction to thermal degradation)
Mean hydrodynamic radius (R_h)	n.d	∼ 20 nm	∼ 10 nm	20 – 40 nm		
MHS, a	n.d	0.75 to 1	∼ 0.9	0.75 to 0.85		
Allomorphic structure	Cellulose I	Cellulose II	Cellulose I	Cellulose I	Low	Cellulose II is more reactive to thermal decomposition, without any influence in the final solid mass loss
Presence of amorphous areas/ crystallinity	Crystalline structure with amorphous areas	Amorphous areas at least partially preserved (Leng et al. 2018)	Crystalline structure	Crystalline structure	Intermediate	Amorphous regions might be less stable and suffer thermal degradation from lower torrefaction temperatures

[a]According to the literature (Hunt et al. 1956; Krässig 1993; Sixta 2008)

[b]Except beech cellulose

[c]A difference of at least one order of magnitude is required to see an impact of the degree of polymerization in the torrefaction behavior

[d]n.d.: not determined

(after CCE). On the contrary, Avicel microcrystalline cellulose presents a significant content in xylose and mannose. This proves the efficacy of CCE in removing hemicellulose residual sugars.

By comparing torrefaction experiments until 300 °C and 350 °C, differences can be clearly appreciated about the temperature around which the main decomposition occurs for each sample. In the case of

Avicel microcrystalline cellulose, the whole peak of the degradation appears at the 300 °C isothermal step, while for the other cellulosic samples it is only completely visualized in torrefaction until 350 °C. At 300 °C, the deceleration in Avicel microcrystalline cellulose after the maximum degradation rate is slower than in torrefaction until 350 °C, which indicates that higher temperatures enhance its decomposition. The degradation of Avicel microcrystalline cellulose at lower temperatures can be at least partly explained by the presence of trace hemicelluloses, particularly because they are xylans-type. Indeed, contrary to Avicel, the low percentage of mannose in ash-wood and pine extracted celluloses does not seem to induce a significant change in their degradation profiles compared to the other extracted celluloses. One possible reason for this behavior is the combination of glucose and mannose in glucomannans in coniferous wood. This agrees with previous studies in the literature with pointed out xylan as the most reactive type of hemicelluloses (Prins et al. 2006).

Molar mass distribution (MMD)

Differences were also observed in degradation profiles of pure cellulosic samples with the same allomorphic structure, such as extracted celluloses and Avicel cellulose (after CCE). That is the reason why molar mass distribution and hydrodynamic behavior are suspected to play an important role on cellulose thermal degradation in torrefaction.

CL are pure cellulose I samples with different average degrees of polymerization (DPw between 1937 and 757). Their degradation profiles in torrefaction are in general very similar. The starting degradation temperature seems to be slightly lower when DPw decreases. In the case of pure cellulose II samples, the behavior of extracted celluloses and Avicel cellulose (after CCE) is rather similar, with small deviations below 300 °C and in the starting degradation temperature. These samples present a factor between 2 and 4 in their DPw values, as well as differences in their MMD. These results suggest that a lower DP may imply a beginning of a significant thermal decomposition of cellulose from sensibly lower temperatures. However, as for all samples the DP remains much lower than that of native cellulose in biomass ($\sim$ 10 000), one should consider that the exact starting temperature for cellulose degradation in native

biomass remains at least partially unknown. Probably at least an order of magnitude of the DPw would be required to see an effect of DP in cellulose behavior in torrefaction, as for example between the raw CL (DPw = 1937) and Avicel cellulose samples (DPw around 100). However, these two samples present different allomorphic structure and/or polysaccharide composition, which may impact cellulose reactivity.

Avicel untreated (microcrystalline) and treated (after CCE) cellulose samples present an equivalent DPw around 100, but a different allomorphic structure and important differences on their MMD. These results lead to think that differences in MMD have a higher impact in cellulose behavior in torrefaction than the average DP and the allomorphic structure, which finally lead to equivalent solid mass loss when cellulose transformation is completely observed. Acid hydrolysis for producing Avicel microcrystalline cellulose probably brought an important chain size reduction, represented by a second peak at low DP values in the MMD curve, as well as size heterogeneity, represented by a large MMD curve. This probably yields to a thermal behavior around 300 °C close to that of hemicelluloses, due to their similar chain length, despite their globally amorphous structure, which contrasts with the high crystallinity reported for Avicel commercial cellulose. The important percentage of very small chains in Avicel microcrystalline cellulose might contribute to enhance its degradation at 300 °C, once the crystalline structure is weakened (Leng et al. 2018). On the contrary, the narrower MMD (lower dispersity) of the extracted celluloses compared to the dispersity of Avicel might indicate that in biomass extracted fractions, cellulose chains with more uniform length would behave more similarly, which could be an explanation for their slower, more progressive degradation.

Hydrodynamic behavior

The selected extraction procedure for obtaining extracted cellulose favors the preservation of the structure of cellulose, namely amorphous regions and cross-links among cellulose chains, while short chains and residual hemicelluloses are removed. However, lower a-values in the MHS curve were obtained for extracted celluloses from hardwood compared to those from agricultural biomass and softwood. In the first case, hardwood cellulose hydrodynamic behavior

would be close to that of CL, characterized by presence of small chains and cross-links. This probably limits the flexibility of the main cellulose chains and impacts the ability of the polymer to be volumetrically expanded. In the second case, agricultural biomass and softwood celluloses hydrodynamic parameters suggest that small cellulose chains and cross-links would be fully removed, leading to a more homogeneous length and higher flexibility and freeness of the polymer chains. Similar MHS parameters were found for Avicel microcrystalline cellulose, where the presence of hemicellulose residues and the mixture of different chain lengths rigidifies the structure and limits, to a certain extent, the flexibility of the chains.

These observations suggest that the hydrodynamic behavior may have global impact on the ability of the polymer structure to react to the thermal degradation. The preservation of cross-links between cellulose chains and the elimination of small chains, at least partially generated in the extraction procedure, as well as residual hemicellulose chains, lead to a pure cellulose structure whose structure and behavior in torrefaction is expected to be close to that of native cellulose in biomass.

Presence of amorphous areas/crystallinity

The cold caustic extraction (CCE) treatment applied in our extraction procedure was reported to preserve amorphous areas in cellulose. On the contrary, the acid hydrolysis treatment to obtain the Avicel microcrystalline cellulose only preserves crystalline cellulose chains (Sixta 2008). As the extracted celluloses were composed of cellulose II, the crystallinity index could not be calculated. In fact, recent studies showed the challenge of this operation (Nomura et al. 2020). Considering that amorphous regions were at least partially preserved in the extracted celluloses and not in the Avicel cellulose, might also explain, together with differences in DP, that extracted celluloses started to degrade from lower temperatures than Avicel cellulose. Amorphous regions might be less stable and suffer an earlier degradation through torrefaction, which is in agreement with previous studies in the literature (Leng et al. 2018).

It is difficult to argue whether the presence of amorphous cellulose has a more considerable impact on cellulose degradation temperature than the

difference in DP between extracted celluloses and Avicel cellulose. In raw biomass samples, the higher DP of cellulose might shift its starting degradation temperature to higher values than those observed for the extracted fractions (below 300 °C). The observed remaining solid mass profiles, exhibiting a progressive solid mass loss which is not accelerated at 300 °C in the isothermal step (Fig. 6), would remain similar but their starting temperature might be shifted to higher values in the case of native cellulose in biomass.

Conclusions

This work showed the influence in cellulose behavior in torrefaction of diverse cellulose properties, namely sample purity in glucose (and trace of hemicellulose sugars), allomorphic structure, average degree of polymerization (DP) and chain length distribution (MMD) and hydrodynamic parameters (intrinsic viscosity, mean hydrodynamic radius). Five cellulose samples extracted from woody and agricultural biomass, four pure cellulose samples from raw and processed purified cotton linter pulps (CL) and two Avicel cellulose samples were characterized in terms of molecular properties and degradation profile in torrefaction.

Torrefaction degradation profiles were very different for the samples analyzed, especially at 300 °C. To explain these differences, the overall results were linked to cellulose characterization, which allowed to suggest the nature and the extent of the impact of cellulose properties on its behavior in torrefaction (Table 4).

The heterogeneity in molar mass distribution strongly impacted cellulose torrefaction. Particularly, the presence of short cellulose chains switched the degradation rate peak to lower temperatures. Furthermore, the presence of hemicellulose residual sugars, especially xylan, increased the reactivity of the sample by inducing a strong acceleration in the degradation rate at 300 °C. These two parameters showed the weaknesses of Avicel microcrystalline cellulose to be considered as a representative model of the cellulose behavior in torrefaction.

The change in cellulose allomorphic structure when obtaining extracted celluloses increased the reactivity of the cellulose sample in torrefaction. However, it did not impact the final solid mass loss in torrefaction.

Furthermore, extracted celluloses presented in general a high purity in glucose and a low dispersity, this is, a narrow molar mass distribution centered at higher DP values than Avicel cellulose. CL samples experiments results showed that a significant difference in the DP is required to impact cellulose behavior in torrefaction. According to previous studies in the literature, the CCE treatment would at least partially preserve amorphous regions in extracted cellulose. These regions would be less stable, which explains the lower starting degradation temperature of extracted celluloses compared to other high crystalline samples, such as commercial Avicel and CL.

According to these results, it can be concluded that the cellulosic samples obtained through the proposed extraction procedure constitute a more representative model of the cellulose behavior in torrefaction than commercial microcrystalline cellulose or to purified CL samples. The main reasons of that are their high purity in glucose, low dispersity, acceptable DP and hydrodynamic behavior, acceptable allomorphic structure and probably the preservation of amorphous areas from native cellulose. The high crystallinity, high dispersity and high percentage of short cellulose chains and xylan residues in commercial cellulose strongly conditioned its behavior in torrefaction.

Declaration

Conflicts of interest The authors declare no conflict of interest.

References

Agrawal RK (1988a) Kinetics of reactions involved in pyrolysis of cellulose I. The three reaction model. Can J Chem Eng 66:403–412. https://doi.org/10.1002/cjce.5450660309

Agrawal RK (1988b) Kinetics of reactions involved in pyrolysis of cellulose II. The modified kilzer-bioid model. Can J Chem Eng 66:413–418. https://doi.org/10.1002/cjce.5450660310

Arseneau DF (1971) Competitive reactions in the thermal decomposition of cellulose. Can J Chem 49:632–638. https://doi.org/10.1139/v71-101

Berggren R, Berthold F, Sjöholm E, Lindström M (2003) Improved methods for evaluating the molar mass distributions of cellulose in kraft pulp. J Appl Polym Sci 88:1170–1179. https://doi.org/10.1002/app.11767

Biagini E, Barontini F, Tognotti L (2006) Devolatilization of biomass fuels and biomass components studied by TG/FTIR technique. Ind Eng Chem Res 45:4486–4493. https://doi.org/10.1021/ie0514049

Bradbury AGW, Sakai Y, Shafizadeh F (1979) A kinetic model for pyrolysis of cellulose. J Appl Polym Sci 23:3271–3280. https://doi.org/10.1002/app.1979.070231112

Broido A, Nelson MA (1975) Char yield on pyrolysis of cellulose. Combust Flame 24:263–268. https://doi.org/10.1016/0010-2180(75)90156-X

Broström M, Nordin A, Pommer L et al (2012) Influence of torrefaction on the devolatilization and oxidation kinetics of wood. J Anal Appl Pyrol 96:100–109. https://doi.org/10.1016/j.jaap.2012.03.011

Chen W-H, Kuo P-C (2011a) Torrefaction and co-torrefaction characterization of hemicellulose, cellulose and lignin as well as torrefaction of some basic constituents in biomass. Energy 36:803–811. https://doi.org/10.1016/j.energy.2010.12.036

Chen W-H, Kuo P-C (2011b) Isothermal torrefaction kinetics of hemicellulose, cellulose, lignin and xylan using thermogravimetric analysis. Energy 36:6451–6460. https://doi.org/10.1016/j.energy.2011.09.022

Chen W-H, Peng J, Bi XT (2015) A state-of-the-art review of biomass torrefaction, densification and applications. Renew Sustain Energy Rev 44:847–866. https://doi.org/10.1016/j.rser.2014.12.039

Chen D, Gao A, Cen K et al (2018) Investigation of biomass torrefaction based on three major components: Hemicellulose, cellulose, and lignin. Energy Convers Manage 169:228–237. https://doi.org/10.1016/j.enconman.2018.05.063

Cheng K, Winter WT, Stipanovic AJ (2012) A modulated-TGA approach to the kinetics of lignocellulosic biomass pyrolysis/combustion. Polym Degrad Stab 97:1606–1615. https://doi.org/10.1016/j.polymdegradstab.2012.06.027

Detcheberry M, Destrac P, Massebeuf S et al (2016) Thermodynamic modeling of the condensable fraction of a gaseous effluent from lignocellulosic biomass torrefaction. Fluid Phase Equilib 409:242–255. https://doi.org/10.1016/j.fluid.2015.09.025

Giudicianni P, Cardone G, Ragucci R (2013) Cellulose, hemicellulose and lignin slow steam pyrolysis: Thermal decomposition of biomass components mixtures. J Anal Appl Pyrol 100:213–222. https://doi.org/10.1016/j.jaap.2012.12.026

Gomez LD, Steele-King CG, McQueen-Mason SJ (2008) Sustainable liquid biofuels from biomass: the writing's on the walls. New Phytol 178:473–485. https://doi.org/10.1111/j.1469-8137.2008.02422.x

González Martínez M, Dupont C, Thiery S et al (2016) Characteristic time analysis of biomass torrefaction phenomena—application to thermogravimetric analysis device.

Chem Eng Trans 50:61–66. https://doi.org/10.3303/CET1650011

González Martínez M, Ohra-aho T, da Silva PD et al (2019) Influence of step duration in fractionated Py-GC/MS of lignocellulosic biomass. J Anal Appl Pyrol 137:195–202. https://doi.org/10.1016/j.jaap.2018.11.026

González Martínez M, Dupont C, da Silva PD et al (2020) Understanding the torrefaction of woody and agricultural biomasses through their extracted macromolecular components. Part 1: experimental thermogravimetric solid mass loss. Energy 205:118067. https://doi.org/10.1016/j.energy.2020.118067

Harmsen PFH, Huijgen WJJ, Bermúdez López LM, Bakker RRC (2010) Literature review of physical and chemical pretreatment processes for lignocellulosic biomass. Energy Research Centre of the Netherlands, Petten

Hosoya T, Kawamoto H, Saka S (2007) Cellulose–hemicellulose and cellulose–lignin interactions in wood pyrolysis at gasification temperature. J Anal Appl Pyrol 80:118–125. https://doi.org/10.1016/j.jaap.2007.01.006

Hunt ML, Newman S, Scheraga HA, Flory PJ (1956) Dimensions and hydrodynamic properties of cellulose trinitrate molecules in dilute solution. J Phys Chem 60:1278–1290. https://doi.org/10.1021/j150543a031

Ioelovich M, Leykin A (2009) Accesibility and supermolecular structure of cellulose. Cellul Chem Technol 43:379–385

Katō K, Komorita H (1968) Pyrolysis of cellulose. Agric Biol Chem 32:21–26. https://doi.org/10.1080/00021369.1968.10859016

Kleen M, Gellerstedt G (1991) Characterization of chemical and mechanical pulps by pyrolysis—gas chromatography/mass spectrometry. J Anal Appl Pyrol 19:139–152. https://doi.org/10.1016/0165-2370(91)80040-F

Kolpak FJ, Blackwell J (1976) Determination of the structure of cellulose II. Macromolecules 9:273–278. https://doi.org/10.1021/ma60050a019

Krässig HA (1993) Cellulose, structure, accessibility and reactivity. Gordon and Breach Publishers, London

Leng E, Zhang Y, Peng Y et al (2018) In situ structural changes of crystalline and amorphous cellulose during slow pyrolysis at low temperatures. Fuel 216:313–321. https://doi.org/10.1016/j.fuel.2017.11.083

Luo W, Liao C (2004) Mechanism study of cellulose rapid pyrolysis. Ind Eng Chem Res 43:5605–5610. https://doi.org/10.1021/ie030774z

Mamleev V, Bourbigot S, Yvon J (2007) Kinetic analysis of the thermal decomposition of cellulose: the main step of mass loss. J Anal Appl Pyrol 80:151–165. https://doi.org/10.1016/j.jaap.2007.01.013

Nocquet T, Dupont C, Commandre J-M et al (2014) Volatile species release during torrefaction of biomass and its macromolecular constituents: part 2—modeling study. Energy 72:188–194. https://doi.org/10.1016/j.energy.2014.05.023

Nomura S, Kugo Y, Erata T (2020) 13C NMR and XRD studies on the enhancement of cellulose II crystallinity with low concentration NaOH post-treatments. Cellulose 27:3553–3563. https://doi.org/10.1007/s10570-020-03036-6

Pasangulapati V, Ramachandriya KD, Kumar A et al (2012) Effects of cellulose, hemicellulose and lignin on thermochemical conversion characteristics of the selected biomass. Biores Technol 114:663–669. https://doi.org/10.1016/j.biortech.2012.03.036

Pastorova I, Botto RE, Arisz PW, Boon JJ (1994) Cellulose char structure: a combined analytical Py-GC-MS, FTIR, and NMR study. Carbohyd Res 262:27–47. https://doi.org/10.1016/0008-6215(94)84003-2

Paulsen AD, Mettler MS, Dauenhauer PJ (2013) The role of sample dimension and temperature in cellulose pyrolysis. Energy Fuels 27:2126–2134. https://doi.org/10.1021/ef302117j

Pena CA, Soto A, King AWT, Rodríguez H (2019) Improved reactivity of cellulose via its crystallinity reduction by nondissolving pretreatment with an ionic liquid. ACS Sustainable Chem Eng 7:9164–9171. https://doi.org/10.1021/acssuschemeng.8b06357

Pisupati SV, Tchapda AH (2015) Chapter 15: thermochemical processing of biomass. In: Advances in bioprocess technology. Pogaku Ravindra, Switzerland

Prins MJ, Ptasinski KJ, Janssen FJJG (2006) Torrefaction of wood: part 1. Weight loss kinetics. J Anal Appl Pyrol 77:28–34. https://doi.org/10.1016/j.jaap.2006.01.002

Ramiah MV (1970) Thermogravimetric and differential thermal analysis of cellulose, hemicellulose, and lignin. J Appl Polym Sci 14:1323–1337. https://doi.org/10.1002/app.1970.070140518

Scheller HV, Ulvskov P (2010) Hemicelluloses. Annu Rev Plant Biol 61:263–289. https://doi.org/10.1146/annurev-arplant-042809-112315

Sczostak A (2010) Cotton Linters: An Alternative cellulosic raw material. Macromol Symp 294:151–151. https://doi.org/10.1002/masy.201050606

Shen DK, Gu S (2009) The mechanism for thermal decomposition of cellulose and its main products. Biores Technol 100:6496–6504. https://doi.org/10.1016/j.biortech.2009.06.095

Shen DK, Gu S, Bridgwater AV (2010) The thermal performance of the polysaccharides extracted from hardwood: cellulose and hemicellulose. Carbohyd Polym 82:39–45. https://doi.org/10.1016/j.carbpol.2010.04.018

Sixta H (2008) Pulp Purification. In: Handbook of pulp. Wiley, pp 933–965

Sjöström E (1993) Wood chemistry: fundamentals and applications, 2nd edn. Academic Press, Cambridge

European Commission (2014) State of play on the sustainability of solid and gaseous biomass used for electricity, heating and cooling in the EU

Stefanidis SD, Kalogiannis KG, Iliopoulou EF et al (2014) A study of lignocellulosic biomass pyrolysis via the pyrolysis of cellulose, hemicellulose and lignin. J Anal Appl Pyrol 105:143–150. https://doi.org/10.1016/j.jaap.2013.10.013

Vea EB, Romeo D, Thomsen M (2018) Biowaste valorisation in a future circular bioeconomy. Procedia CIRP 69:591–596. https://doi.org/10.1016/j.procir.2017.11.062

Wang S, Guo X, Liang T et al (2012) Mechanism research on cellulose pyrolysis by Py-GC/MS and subsequent density functional theory studies. Biores Technol 104:722–728. https://doi.org/10.1016/j.biortech.2011.10.078

Wang Z, McDonald AG, Westerhof RJM et al (2013) Effect of cellulose crystallinity on the formation of a liquid intermediate and on product distribution during pyrolysis.

J Anal Appl Pyrol 100:56–66. https://doi.org/10.1016/j.jaap.2012.11.017

Williams PT, Besler S (1996) The influence of temperature and heating rate on the slow pyrolysis of biomass. Renew Energy 7:233–250. https://doi.org/10.1016/0960-1481(96)00006-7

Wooten JB, Seeman JI, Hajaligol MR (2004) Observation and characterization of cellulose pyrolysis intermediates by 13C CPMAS NMR. New Mech Model Energy Fuels 18:1–15. https://doi.org/10.1021/ef0300601

Yang H, Yan R, Chen H et al (2007) Characteristics of hemi-cellulose, cellulose and lignin pyrolysis. Fuel 86:1781–1788. https://doi.org/10.1016/j.fuel.2006.12.013